$1/\sigma$ expansion for quantum percolation

A. B. Harris
Schlumberger-Doll Research, P.O. Box 307, Ridgefield, Connecticut 06877
and Department of Physics, University of Pennsylvania, Philadelphia, Pennsylvania 19104
(Received 28 April 1983)

A method for obtaining a $1/\sigma$ expansion for certain statistical models is presented, where $\sigma+1$ is the coordination number of the lattice. The method depends on being able to generate exact recursion relations for the Cayley tree. By perturbing the recursion relation to take account of the dominant loops in a hypercubic lattice for large σ, we obtain corrections of order σ^{-2} to the recursion relations. For the tight-binding model on random bond clusters (the quantum-percolation problem) we obtain corrections to this order for the critical concentration p^* at which the transition between localized and extended zero-energy eigenfunctions takes place. It is believed that this concentration coincides with the transition when all energies are considered. In addition, we display the relation for the Cayley tree between quantum-percolation and lattice animals (or dilute branched polymers). We show that this relation manifests itself in the appearance of singularities in the quantum-percolation problem at *negative* concentration which correspond to the physical transition at positive fugacity in the statistics of lattice animals. Corrections of order σ^{-2} to the location of this unphysical singularity in the quantum-percolation problem are also obtained.

I. INTRODUCTION

In this paper we develop a method for obtaining expansions for the properties of statistical models on d-dimensional lattices in powers of $1/\sigma$, where $\sigma+1$ is the coordination number of the lattice. This type of expansion has been used in a wide variety of contexts in the past several years.[1-10] One reason we undertake this program is to enable improved series-expansion estimates to be made for the critical exponents of such models. Usually the uncertainty in determining critical exponents by series-expansion techniques is due in large part to the uncertainty in the critical value of the coupling constant (e.g., the temperature). Any independent information which helps fix the critical value of the coupling constant is therefore of interest. Previously,[10] we have given a method for evaluating this critical value as a power series in $1/\sigma$ for a wide class of statistical-mechanical models to which the original method[3] could not conveniently be applied. In the present paper we wish to carry out such a calculation for the quantum-percolation model, which describes quantum hopping on percolation clusters. Since this model has not yet been formulated in terms of partition function or any convenient field-theoretic expression, the methods of Refs. 3 and 10 are not immediately applicable, and furthermore direct construction of the $1/\sigma$ expansion seems to be impractical. Accordingly, we present here a new approach to the calculation of this expansion, one which can be used if an exact recursive solution for the Cayley tree (see Fig. 1) is available.

To locate the critical value of the coupling constant at a continuous transition as a series in $1/\sigma$ we need to construct a series in $1/\sigma$ for a susceptibility χ whose divergence characterizes the critical point. A convenient procedure is to expand the susceptibility for the hypercubic lattice $\chi_{\rm HC}(\sigma)$ about the corresponding value $\chi_{\rm CT}(\sigma)$ for a Cayley tree having the same coordination number, $\sigma+1$. Thus we write

$$\chi_{\rm HC}(\sigma)=\chi_{\rm CT}(\sigma)+\sum_{n=2}^{\infty}\sigma^{-n}\chi^{(n)}\,. \tag{1.1}$$

Here we noted the fact that the leading term in $\chi_{\rm HC}-\chi_{\rm CT}$ may be attributed to the most important diagrams by which the d-dimensional hypercubic lattice differs from the Cayley tree, namely diagrams with a single square loop to each vertex of which arbitrarily complicated trees are attached. The weight of these diagrams relative to those with no loops is of order σ^{-2}, so that $\chi^{(n)}=0$ for $n<2$. In principle, the calculation of $\chi^{(n)}$ for $n\geq 2$ can be effected by explicit consideration of diagrams with successively more, larger, or more strongly interconnected loops. In the case of quantum percolation, which we consider here, such a direct enumeration does not seem feasible. Instead we propose a method in which loops in the hyper-

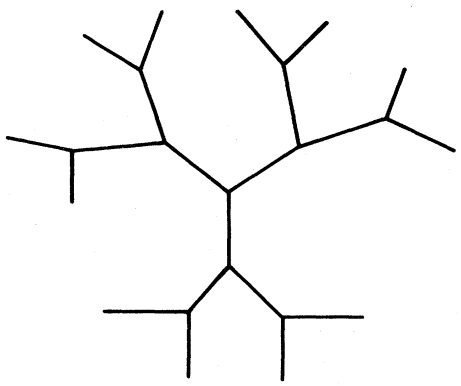

FIG. 1. Section of a Cayley tree of coordination number $z=\sigma+1=3$.

 ©1984 The American Physical Society

cubic lattice are included by perturbing the recursion relations, which determine the susceptibility for the Cayley tree. To test and illustrate the method we first display it for the percolation problem, where the expansion for the critical percolation concentration p_c has been previously worked out to high order.[9] We then apply the method to a suitably defined localization susceptibility of the quantum-percolation problem. We determine the leading correction of order $(1/\sigma)^2$ for the critical concentration p^* where $\chi(p)$ diverges. Even this low-order result is helpful for current series investigations of the quantum-percolation problem which are aimed at determining the marginal dimension d_c at which mean-field theory breaks down (d_c is probably not less than 6, so that $\sigma^{-2}\sim 10^{-2}$). Calculations to higher order in $1/\sigma$ could be undertaken but they rapidly become complicated.

An important feature of the method used here is that the determination of p^* depends on locating the singularity in χ rather than analyzing the large-σ behavior of the ratio of successive terms in the expansion of χ in powers of p. In fact, for quantum percolation the use of such a ratio method to locate p^* would fail completely since the singularity in $\chi(p)$ closest to the origin in the complex p plane occurs for an unphysical negative value of the concentration, $\hat{p}$. This singularity in $\chi(p)$ is weaker than the physical one at positive p and its existence may be further evidence of a close connection[11–13] between the critical properties of the mobility edge in the localization problem and the critical properties of lattice animals,[14] since the mean-field (i.e., Cayley-tree) equations for quantum percolation at concentration p are identical to those for lattice animals at fugacity $K=-p$ (see Appendix A).

Briefly this paper is organized as follows. In Sec. II we present the method and apply it to the percolation problem. This application serves both as a test and an illustration of the method. In Sec. III we describe quantum percolation by a hopping model in which hopping over occupied nearest-neighbor bonds is confined to percolation clusters which occur when the concentration of randomly occupied bonds is p. We introduce a localization susceptibility χ which diverges when any of the zero-energy eigenfunctions become extended. This susceptibility is related to a participation ratio (i.e., the fourth power of the modulus of the wave function) and has not been formulated in terms of a partition function or an action, so that the method of Sec. II must be used. In Sec. IV we give some of the calculations from which the critical concentration p^*, for the onset of extended states, and the unphysical negative concentration $\hat{p}<0$, where the susceptibility is also singular, can be obtained to order $(1/\sigma)^2$. Our conclusions are summarized in Sec. V.

II. HYPERCUBIC LATTICE AS A PERTURBATION OF THE CAYLEY TREE

We now discuss the expansion in powers of concentration p for some bulk thermodynamic property $G(p)$ which is usually a susceptibility of some type of a randomly dilute system of bonds. For definiteness we assume $G(p)$ to be of the form

$$G(p)=\sum_{x,x'}[\chi(x,x')]_p \equiv Ng(p)\ , \tag{2.1}$$

where $\chi(x,x')$ is a correlation function associated with sites x and x' which is nonzero if and only if sites x and x' are in the same cluster and $[\ ]_p$ denotes an average over configurations of randomly occupied bonds at fixed concentration p. Also N is the total number of lattice sites, so that $g(p)$ is the susceptibility per site. To construct the concentration expansion it is, of course, assumed that for any connected set of bonds, Γ, we can calculate the associated value of G, denoted $G(\Gamma)$. In principle, we can express $G(p)$, as a sum over the values of G for all clusters of bonds, weighting each term by the probability of occurrence $P(\Gamma)$ of the cluster Γ, which is given by

$$P(\Gamma)=p^{n_b(\Gamma)}(1-p)^{n_p(\Gamma)}\ , \tag{2.2}$$

where $n_b(\Gamma)$ is the number of occupied bonds in the cluster Γ, and $n_p(\Gamma)$ is the number of perimeter bonds which must be vacant in order to define the boundary of the cluster Γ. Thus the power-series expansion of $g(p)$ assumes the form

$$g(p)=\sum_{\Gamma} p^{n_b(\Gamma)} w(\Gamma) G_c(\Gamma)\ , \tag{2.3}$$

where $w(\Gamma)$ is the number of ways per site that the cluster Γ can occur on the lattice, and $G_c(\Gamma)$ is the cumulant value of G for the cluster Γ defined recursively via

$$G_c(\Gamma)=G(\Gamma)-\sum_{\gamma\subset\Gamma} G_c(\gamma)\ , \tag{2.4}$$

where the sum is over all connected proper subclusters γ contained within Γ. The weak embedding constant $w(\Gamma)$ can be expressed as a polynomial of degree $n_b(\Gamma)$ in d. The two highest-order terms in this polynomial are the same for the d-dimensional hypercubic lattice and the Cayley tree with the same coordination number. Because of this, the Cayley tree gives the high-dimensionality limit for the hypercubic lattice in the sense of Eq. (1.1). The terms in $w(\Gamma)$ of order $d^{n_b(\Gamma)-2}$ are different for the Cayley tree and for the hypercubic lattice because of the occurrence of squares, i.e., loops leads of four bonds, which can occur on the cubic lattices but not on the tree and these corrections determine $\chi^{(2)}$ in Eq. (1.1). The occurrence of larger single loops or of multiple loops leads to effects of still lower order in d and enter the calculation of $\chi^{(n)}$ for $n>2$.

In principle, then, these correction terms could be determined by solving exactly and summing over all diagrams consisting of a square to whose vertices are appended arbitrary trees (see Fig. 2). An alternative approach is more fruitful. We consider the exact solution for the Cayley tree as obtained by a recursion relation in which the Cayley tree is built up by sequentially adding shells of neighbors around a central origin. We then include diagrams like those in Fig. 2 by perturbing these recursion relations. To see that we can indeed describe diagrams with a single loop by a recursion relation, we imagine building the cluster in Fig. 2 outward from the origin, labeled "*O*." The perturbation is described by modifying the recursion relation for site "*b*," which for arbitrary diagrams of this

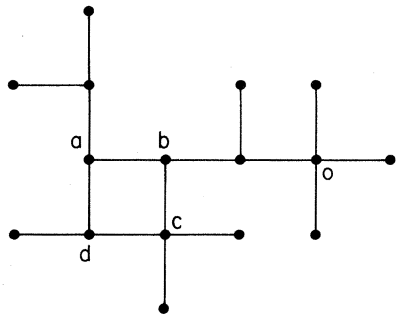

FIG. 2. Example of a square (a,b,c,d) with trees appended to each vertex. Origin is marked O, and b is the site at which the recursion relation for the Cayley tree must be modified to generate the square loop.

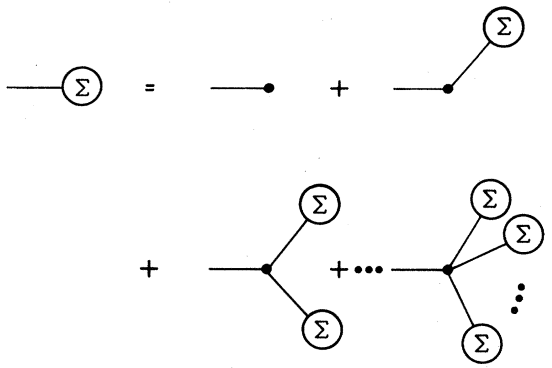

FIG. 3. Schematic representation of the recursion relation of Eq. (2.8).

type, of course, could be any site on the tree.

To illustrate our approach we will start by applying it to the percolation problem where the details are very simple and the result well known. Let Γ_0 be a diagram containing the origin and consider the generating function[15]

$$F(p,q)=\sum_{\Gamma_0} P(\Gamma_0) q^{n_s(\Gamma_0)} , \tag{2.5}$$

where $n_s(\Gamma_0)$ is the number of sites in the cluster Γ_0. From F we can obtain the percolation susceptibility per site $\chi(p)$ as

$$\chi(p)=\left.\frac{\partial F(p,q)}{\partial q}\right|_{q=1} , \tag{2.6}$$

so that the percolation susceptibility is identified as the mean cluster size. To obtain $F(p,q)$ exactly we write[15]

$$F(p,q)=q[1-p+qp\Sigma(p,q)]^{\sigma+1} , \tag{2.7}$$

where $\Sigma(p,q)$ is a vertex function which includes the contribution to $F(p,q)$ from one vertex of the tree and all that is appended to it. The factor q is used to count sites in the cluster and the factors p and $1-p$ are the factors in $P(\Gamma_0)$ associated with an occupied bond and an unoccupied bond, respectively. The recursion relation for Σ is

$$\Sigma(p,q)=[1-p+qp\Sigma(p,q)]^{\sigma} , \tag{2.8a}$$

which we may express as

$$\Phi(\Sigma)=0 . \tag{2.8b}$$

If $\Phi_0(\Sigma)$ denotes the value of $\Phi(\Sigma)$ for the Cayley tree, then Eq. (2.8a) indicates that

$$\Phi_0(\Sigma)=[1-p+qp\Sigma(p,q)]^{\sigma}-\Sigma(p,q)=0 . \tag{2.8c}$$

Schematically, Eq. (2.8a) may be represented as shown in Fig. 3. The definition of Eq. (2.5) shows that $F(p,q=1)$ is a normalization sum, and with Eq. (2.7) or from Eq. (2.8), one can show that

$$\Sigma(p,1)=1 . \tag{2.9}$$

From Eq. (2.6) we see that the singularity in $\chi(p)$ is due to the singularity in $\partial\Sigma/\partial q$, which we evaluate by

$$\frac{\partial\Sigma}{\partial q}=-\left[\frac{\partial\Phi(\Sigma,q)/\partial q}{\partial\Phi(\Sigma,q)/\partial\Sigma}\right] . \tag{2.10}$$

Thus the critical point is determined by simultaneously solving Eq. (2.8b) and

$$\frac{\partial\Phi(\Sigma,q)}{\partial\Sigma}=0 . \tag{2.11}$$

In agreement with the known results[15] we thereby obtain the critical percolation concentration p_c as $p_c=\sigma^{-1}$. When we allow for the addition of a single square to the structure of the Cayley tree, Eq. (2.7) will be revised. However, the singularity in $\chi(p)$ can still be located by solving simultaneously Eqs. (2.8b) and (2.11), provided we include the perturbative contribution to $\Phi(\Sigma)$ due to a square.

We now construct the perturbation to Φ by considering the effects of the difference between the Cayley tree and the hypercubic lattice. There are three types of correction terms. In the first type, illustrated in Fig. 4, the probability factor of the diagram is incorrectly given by the Cayley tree. The second type of correction is due to square loops, which of course do not occur on the Cayley tree (see Fig. 5). Finally, in the third type, illustrated in Fig. 6, we include the contribution to Φ due to diagrams which can

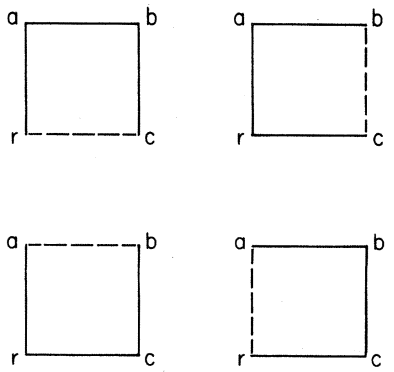

FIG. 4. Diagrams appended to the root vertex r which are incorrectly treated on the hypercubic lattice by the recursion relations for the Cayley tree. Dashed line represents an unoccupied bond which is a common neighbor to two sites in the diagram.

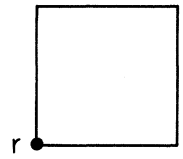

FIG. 5. Diagram, the square loop, which can not occur on the Cayley tree, but which yields the dominant correction for the hypercubic lattice.

occur on the Cayley tree, but whose connectivity would be different on a real hypercubic lattice. We construct corrections to the recursion relation for $\Sigma(p,q)$ for the root vertex labeled r in these figures. For instance, if Eq. (2.8a) is iterated several times, we obtain diagrams, some of which are of the type shown in Fig. 4, where the sites connected by dashed lines would have distinct neighboring (unoccupied) perimeter bonds on the Cayley tree, giving rise to a factor $(1-p)^2$. In contrast, on the hypercubic lattice these two bonds are not distinct if the points shown actually form a square and therefore give rise to a factor $1-p$. To correct this we include, in the Cayley-tree result, the factor $-(1-p)^2+(1-p)=p(1-p)$. If we write

$$\Phi=\Phi_0+\delta\Phi\ , \tag{2.12}$$

where Φ_0 is the Cayley-tree value of Φ given in Eq. (2.8), then the sum of the contributions to $\delta\Phi$ from the diagrams of Fig. 4, which we indicate by a superscript (4) on $\delta\Phi$, is

$$[\delta\Phi(\Sigma,q)]^{(4)}=4\frac{(\sigma-1)^2}{2}p^3q^3[p(1-p)] \times[1-p+pq\Sigma(p,q)]^{4\sigma-5}\ . \tag{2.13}$$

Here the factor $(\sigma-1)^2/2$ is the number of ways a square can be attached to the branch at site r. The factors p^3 and q^3 are due to an addition from site r of three occupied bonds and three occupied sites, respectively. The factor $1-p+pq\Sigma(p,q)$ is added whenever there is a branch which may be occupied $[pq\Sigma(p,q)]$, or may not be occupied $(1-p)$. Note that the dashed bond in Fig. 4 must be unoccupied in order for the diagram to have the topology of Fig. 4. Thus the vertices "r," "a," "b," and "c," have, respectively, $\sigma-2$, $\sigma-1$, $\sigma-1$, and $\sigma-1$ bonds, which

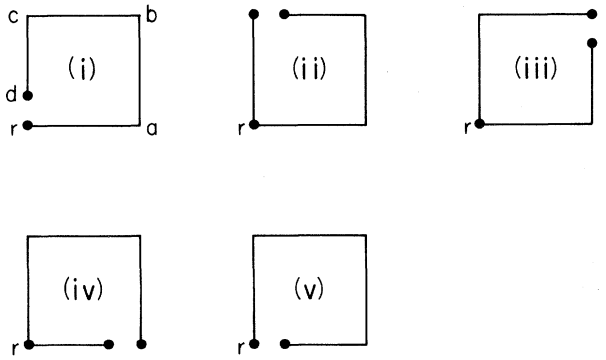

FIG. 6. Diagrams generated from the root vertex r whose connectivity is different when the diagram is transferred from the Cayley tree to the hypercubic lattice.

may or may not be occupied. The factor $p(1-p)$ is the correction factor described above Eq. (2.12).

Next we consider diagrams which cannot occur on the Cayley tree, but which can occur on the hypercubic lattice. These are of the type shown in Fig. 5. The contribution to $\delta\Phi$ from this type of diagram, which we indicate by a superscript (5) on $\delta\Phi$, is

$$[\delta\Phi(\Sigma,q)]^{(5)}=\frac{(\sigma-1)^2}{2}q^3p^4[1-p+pq\Sigma(p,q)]^{4\sigma-5}\ . \tag{2.14}$$

The factors here are similar to those in Eq. (2.13).

Finally, we must subtract the contribution of diagrams which can occur on the Cayley tree but whose topology would be different on the hypercubic lattice. The diagrams are shown in Fig. 6. In diagram (i) of Fig. 6 the vertices "d" and r coincide when the diagram is moved from the Cayley tree to the hypercubic lattice. Similarly, the vertices close to one another in the other diagrams would coincide on the hypercubic lattice. We must now determine the exponent of the factor $1-p+pq\Sigma(p,q)$, which is the total number of surrounding bonds which may or may not be occupied, consistent with the topology of the diagram. In diagram (i) vertices a, b, c, and d have, respectively, $\sigma-1$, $\sigma-1$, $\sigma-1$, and σ such bonds. Vertex r has only $\sigma-2$ such bonds, because if the bond from r to c were occupied, the diagram would be of the type (ii) in the next panel. Thus the bond from r to c must be unoccupied and carry a factor $1-p$. This overcounting difficulty occurs for all types except (v), where no such restriction need be imposed. The contribution to $\delta\Phi$ from the diagrams of Fig. 6, indicated by a superscript (6), is

$$[\delta\Phi(\Sigma)]^{(6)}=-\frac{(\sigma-1)^2}{2}p^4q^4 \times\{4(1-p)[1-p+qp\Sigma(p,q)]^{5\sigma-5} +[1-p+qp\Sigma(p,q)]^{5\sigma-4}\}\ . \tag{2.15}$$

Thus,

$$\delta\Phi(\Sigma)=\frac{(\sigma-1)^2}{2}p^3q^3[1-p+qp\Sigma(p,q)]^{4\sigma-5} \times\{4p(1-p)-4pq(1-p)[1-p+qp\Sigma(p,q)]^{\sigma} +p-pq[1-p+qp\Sigma(p,q)]^{\sigma+1}\}\ . \tag{2.16}$$

We note that for $q=1$, $\Sigma(p,1)=1$ satisfies Eq. (2.8) because

$$\delta\Phi(\Sigma=1)=0\ ,\quad q=1\ . \tag{2.17}$$

This check tests that we have correctly counted the diagrams involved.

In general, the calculation to higher order in $1/\sigma$ rapidly becomes involved with the use of this method. However, we can extend the results to order $(1/\sigma)^3$ for percolation quite easily by carrying out the analogous calculation where the added figure is a six-bond loop rather than a four-bond loop. For an added six-bond loop, the factor

$(\sigma-1)^2/2$ must be replaced by the number of ways a six-bond loop can be added at a given site. To leading order in σ this is $2\sigma^3$. Also, in the various places where 4 enters in Eq. (2.16) one should replace the 4's by 6's. Thus, for six-bonded insertions we have a contribution to $\delta\Phi$ of

$$\delta\Phi=2\sigma^3p^5q^5[1-p+qp\Sigma(p,q)]^{6\sigma-7}\times\{6p(1-p)-6pq(1-p)[1-p+qp\Sigma(p,q)]^{\sigma}+p-pq[1-p+pq\Sigma(p,q)]^{\sigma+1}\}\ . \quad (2.18)$$

Note that Eq. (2.17) holds for this result. To find the perturbed singularity in $\chi(p)$ we use Eq. (2.12) for Φ with $\delta\Phi$ being the sum of the contributions written in Eqs. (2.16) and (2.18). The calculation simplifies considerably because we only need evaluations of $\Sigma(p,1)$ for which Eq. (2.9) is used. Evaluation of Eq. (2.11) yields

$$0=\sigma p_c-1+\frac{(\sigma-1)^2}{2}p_c^3[-4\sigma p_c^2(1-p_c)-p_c^2(\sigma+1)]+2\sigma^3p_c^5[-6\sigma p_c^2(1-p_c)-p_c^2(\sigma+1)]\ , \quad (2.19)$$

which gives, to order σ^{-3},

$$\sigma p_c=1+\frac{5}{2\sigma^2}+\frac{15}{2\sigma^3}+\cdots\ , \quad (2.20)$$

in agreement with the known results.[9] We have been careful in constructing Eq. (2.16) to get the exponents of the factors $1-p+qp\Sigma(p,q)$ correct. However if we had only wanted the result in Eq. (2.30) to order σ^{-2}, we would only have had to evaluate the exponent to leading order in σ, in which case we could simply associate a factor $\Sigma(p,q)$ with each vertex. For the percolation problem the approach used here is not as efficient as the one used in Ref. 9. However, it will prove useful for the quantum-percolation model introduced in the next section.

III. FORMULATION OF THE QUANTUM PERCOLATION PROBLEM

The model of localization we treat is governed by the Hamiltonian[16]

$$H=\sum_{\langle i,j\rangle}t_{ij}(c_i^\dagger c_j+c_j^\dagger c_i)\ , \quad (3.1)$$

where $\langle\ ,\ \rangle$ indicates that the sum is restricted to pairs of nearest-neighbor sites, each pair being counted once, and each nearest-neighbor t_{ij} assumes the values t with probability p and 0 with probability $1-p$. A definition of a localization susceptibility per site $\chi(p)$ for zero-energy eigenstates for the Cayley tree is[17,18]

$$\chi(p)=\sum_{\Gamma_0}P(\Gamma_0)\chi(\Gamma_0)\ , \quad (3.2)$$

where the sum is over all clusters Γ_0 which intersect the origin, and $\chi(\Gamma_0)$ is the susceptibility for the site at the origin from the cluster Γ_0, defined by[19]

$$\chi(\Gamma_0)=\max\left[\sum_{i\subset\Gamma_0}|\psi(i)|^4\right]^{-1}\ , \quad (3.3)$$

where the maximum has been taken over the manifold of zero-energy eigenstates which (a) have nonzero amplitude on the origin, and (b) cannot be decomposed into two or more spatially disjoint zero-energy eigenfunctions. Since the ψ which gives the maximum in Eq. (3.3) has equal amplitude on all sites on which it is nonvanishing,[17] $\chi(\Gamma_0)$ is simply the number of sites in Γ_0 covered by the maximally extended zero-energy eigenstate. Also, in Eq. (3.2), $P(\Gamma_0)$ is the probability for the formation of the cluster Γ_0 given by Eq. (2.1). This definition of $\chi(p)$ must be generalized when nonunimodular solutions result from the maximization of Eq. (3.3), as happens on the hypercubic lattice.[20] However, to the order we consider here, we may continue to use the definition of Eq. (3.3). Thus we are led to consider the generating function

$$F(p,q)=\sum_{\Gamma_0}P(\Gamma_0)q^{\chi(\Gamma_0)}\ , \quad (3.4)$$

so that Eq. (2.6) holds.

Before embarking on a general analysis we will illustrate the calculation of $\chi(\Gamma_0)$ for the cluster of occupied bonds shown in Fig. 7. Recall that a zero-energy eigenfunction $\psi(j)$ satisfies the equation

$$\sum_j t_{ij}\psi(j)=0\ . \quad (3.5)$$

In other words, for any given site i, the sum over the values of the wave function on all neighboring sites connected to site i by an occupied bond must vanish. Thus for the diagram of Fig. 7 we see that any zero-energy eigenfunction must vanish at sites 2, 5, and 10, if we apply Eq. (3.5), taking i to be the sites at the end of a branch (viz., sites 1, 4, and 9). Next we use Eq. (3.5) taking i to be sites 3, 6, and 11. Then we see that the zero-energy eigenfunction vanishes on sites 13, 7, and 12. Finally, we apply Eq. (3.5) to sites 12 and 10, whereby we conclude that any zero-energy eigenfunction vanishes on sites 11 and 9. Thus, in the part of the diagram shown explicitly in Fig. 7 (i.e., in the region which is outside the open circle labeled

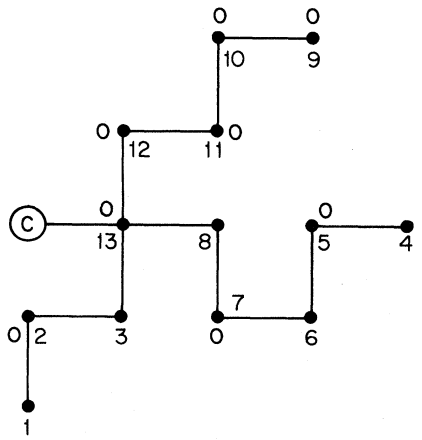

FIG. 7. Cluster of occupied bonds containing a node, site 13, from which three chains emanate. Origin is in the part of the cluster represented schematically by the circle labeled *C*. Sites 1, 3, 4, 6, 8, 9, and 11 are even and sites 2, 13, 5, 7, 10, and 12 are odd. Sites where all zero-energy eigenfunctions must vanish are labeled *O*.

"C" and does not include the bond connecting C to site 13) there are five sites which can be covered by a zero-energy eigenfunction which extends into the circle C. This section can be characterized by a generating function $f(p,q)=p^{12}(1-p)^{13\sigma-12}q^5$, where the factors are p^{12} for the 12 occupied bonds, $(1-p)^{13\sigma-12}$ for the $13\sigma-12$ unoccupied bonds emanating from sites 1, 2, . . . , 13, and q^5 for the five sites over which the wave function can spread. Therefore this section of the diagram contributes a factor of $f(p,q)$ to $F(p,q)$ if the wave function can actually reach the origin located in C, or a factor $f(p,1)$ if the wave function cannot reach the origin. This example shows that we must keep track of how the wave function spreads out from the origin.

The exact solution[17,18,21] for $F(p,q)$ on the Cayley tree is accomplished by a recursion relation similar to that of Eq. (2.8). The recursion relation we seek should be such that it represents the sum over all configurations required in Eq. (3.4). As we build up the cluster by adding bonds outwards from the origin, we will add up to σ occupied bonds at each boundary site. Thus we must consider the 2^σ choices for either occupying or not occupying each of these σ additional bonds. Also, we must include a factor q, when a site is added, which can be covered by a zero-energy eigenfunction which intersects the origin. To implement this method of calculation we need to classify sites as either "even" or "odd" depending on whether or not they can be covered by the required zero-energy eigenfunction. In this connection recall the example of Fig. 7. There, by working inward from the boundary we found that any zero-energy eigenfunction must vanish on sites 2, 13, 6, 8, 10, and 12, and these we will call odd sites. The other sites are even sites. After we finished working inwards to site 13, we subsequently determined that the eigenfunction, in fact, must vanish on the entire branch containing sites 9—13. This will always happen when two odd sites (in this case, sites 12 and 13) are adjacent to one another. It is convenient to take account of this "blocking" effect separately, so that our classification scheme remains a simple one. The general method for classifying sites is accomplished recursively as follows. We work inwards from the boundary towards the origin. All boundary sites are classified as even. As we work inward a given site i is classified as follows. Site i is even if all its outer neighbors are odd, and it is odd if any of its outer neighbors are even. Thus, along a chain, sites alternate between being even and odd. Now consider a node at site s, i.e., a site which has more than one outer neighbor. In particular consider the case when some of its outer neighbors are even and some are odd. (Site 13 in Fig. 7 is an example of such a node.) Then the node is odd according to our classification scheme. As the example in Fig. 7 illustrates, the zero-energy eigenfunction intersecting the origin vanishes on all branches which have an odd site adjacent to the odd node at site s. For such a branch (e.g., sites 9—12 in Fig. 7), we should set $q=1$ since the wave function cannot penetrate that branch.

Since the eigenfunction can only intersect the origin if the orgin has all odd neighbors, the analog of Eq. (2.7) in this case is

$$F(p,q)=q[1-p+p\Sigma_o(p,q)]^{(\sigma+1)}, \tag{3.6}$$

where Σ_o (and later Σ_e) is the contributing factor to $F(p,q)$ from an odd (and later even) vertex. Note that in Eq. (3.6), $\Sigma_o(p,q)$ does not carry a factor q as it would in analogy with Eq. (2.7). This absence is due to the fact that the wave function vanishes on all odd vertices. To construct the recursion relation for Σ we must consider the 3^σ possible conformations as we add bonds to the cluster. Each bond can either be (a) unoccupied, (b) occupied and connected to an even site, or (c) occupied and connected to an odd site. Following this reasoning we find that for the Cayley tree Σ obeys the recursion relations[22]

$$\Phi_e(\Sigma)\equiv[1-p+p\Sigma_o(p,q)]^\sigma-\Sigma_e(p,q)=0\,, \tag{3.7a}$$

$$\Phi_o(\Sigma)\equiv[1-p+qp\Sigma_e(p,q)+p\Sigma_o(p,1)]^\sigma-\Sigma_o(p,q)-[1-p+p\Sigma_o(p,1)]^\sigma=0\,. \tag{3.7b}$$

These relations are shown schematically in Fig. 8 and can be understood as follows. Equation (3.7a) is logically similar to Eq. (2.8) but we include no factor of q because adding an odd site to the root vertex (which is even) does not increase $\chi(\Gamma_0)$, since the wave function vanishes on the additional odd site. Also note that the expansion of $[1-p+p\Sigma_o(p,q)]^\sigma$ in powers of p yields all possible random occupations of bonds such that only odd sites are outside the site being classified. In Eq. (3.7b), for each outgoing branch from an odd root vertex, we may add either no site $1-p$, an odd site $p\Sigma_o$, or an even site $pq\Sigma_e$, and only the latter carries a factor q. However, for the vertex r to be an odd site, at least one even site must be added; hence we subtract the last term in Eq. (3.7b). In Eq. (3.7b) note that the $\Sigma_o(p,q)$'s inside the square brackets are evaluated at $q=1$ since they represent the occurrence of two adjacent odd sites which break the connectivity of the eigenfunction. Also note that for $q=1$

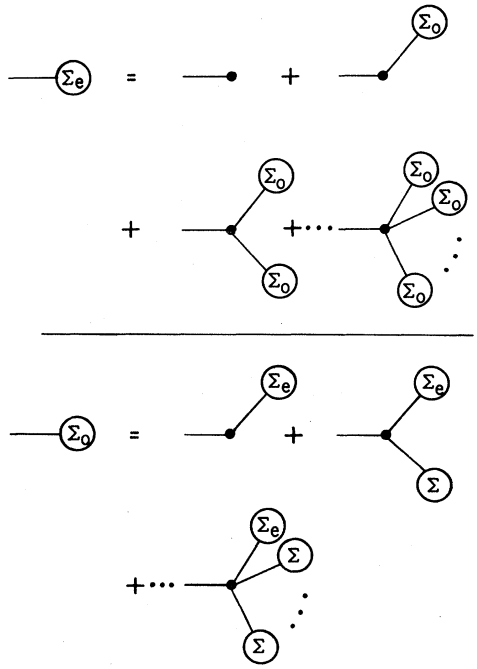

FIG. 8. Schematic representation of the recursion relations, Eq. (3.7). Here Σ denotes $\Sigma_o(p,q)+\Sigma_e(p)$. The factors of q are not represented here.

the quantity $\Sigma_e+\Sigma_o$ satisfies the recursion relation for percolation as expected. Thus, in analogy with Eq. (2.9) we have

$$\Sigma_e(p)+\Sigma_o(p)=1\ , \tag{3.8}$$

where $\Sigma(p)=\Sigma(p,1)$. (This type of notation will be used for other functions of p and q.) We use Eq. (3.7a) to eliminate Σ_e in favor of Σ_o and express Eq. (3.7b) in terms of $\Lambda(p,q)$ defined by

$$\Lambda(p,q)=1-p+p\Sigma_o(p,q)\ . \tag{3.9}$$

Thereby we find

$$\Phi(\Lambda)\equiv\frac{\Lambda(p,q)-(1-p)}{p}$$
$$-[\Lambda(p)+pq\Lambda(p,q)^\sigma]^\sigma+\Lambda(p)^\sigma=0\ . \tag{3.10}$$

Following the argument leading to Eq. (2.11) we see that $\chi(p)$ has a singularity at a critical value of p, denoted p^*, determined by

$$\frac{\partial\Phi(\Lambda)}{\partial\Lambda(p,q)}=0\ . \tag{3.11}$$

For $q=1$, Eqs. (3.10) and (3.11) lead to the relations

$$\Lambda(p)+p\Lambda(p)^\sigma=1\ , \tag{3.12a}$$

$$1=\sigma^2p^2\Lambda(p)^{\sigma-1}\ . \tag{3.12b}$$

From these equations we find that p^* is determined by[18]

$$1+(p^*\sigma^2)^{-1}=(p^*\sigma)^{2/(\sigma-1)}\ . \tag{3.13}$$

For large σ this gives $p^*\sim a/\sigma$, with $a\approx 1.421\,53$. For p near p^* we have

$$\chi(p)\sim(p^*-p)^{-1}\ \text{ as } p\to(p^*)^-\ . \tag{3.14}$$

There are also singularities in $\chi(p)$ at negative p.[23] These come from a singularity in $\Lambda(p)$ which occurs when, for $q=1$, Eq. (3.10) holds and

$$\frac{\partial\Phi(\Lambda)}{\partial\Lambda}=0\ . \tag{3.15}$$

These conditions hold for a certain value of p which we denote $\hat{p}$. Equation (3.15) yields $F_1F_2=0$, with

$$F_1=1-\sigma p[\Lambda(p)+p\Lambda(p)^\sigma]^{\sigma-1}\ , \tag{3.16a}$$

$$F_2=1+\sigma p\Lambda(p)^{\sigma-1}\ . \tag{3.16b}$$

Setting $F_1=0$ and using Eq. (3.12a) gives $\hat{p}=p_c=\sigma^{-1}$, where possible nonanalytic behavior can occur due to the formation of an infinite cluster at the critical percolation concentration p_c. (Actually, there is no nonanalytic behavior in the localization susceptibility of the Cayley tree at the critical percolation concentration.[18]) In conjunction with Eq. (3.12a) setting $F_2=0$ gives a singularity in $\chi(p)$ at $p=\hat{p}$, with

$$\hat{p}=-\frac{1}{\sigma}\left[\frac{\sigma-1}{\sigma}\right]^{\sigma-1}=-K_c\ , \tag{3.17}$$

where K_c is the critical fugacity for lattice animals or dilute branched polymers on a Cayley tree.[9,10] The relation between localization and lattice animals on a Cayley tree is explored in more detail in Appendix A, where it is shown that

$$\chi(p)\approx\chi(\hat{p})+\text{const}\times|p-\hat{p}|^{1/2}\ \text{ as } p\to\hat{p}\ . \tag{3.18}$$

IV. EVALUATION OF CORRECTIONS TO ORDER σ^{-2} FOR QUANTUM PERCOLATION

In principle, the calculation of corrections to $\Phi(\Sigma)$ to order σ^{-2} follows along the lines of the previous calculation in Sec. II for percolation and we outline here only the salient features of the calculation. For instance, we show in Fig. 9 all possible labelings of the diagrams of Fig. 4 which contribute to $\delta\Phi$ and the corresponding contributions to $\delta\Phi_e$ and $\delta\Phi_0$ are listed in Table I. To illustrate the calculations we consider the contribution $\delta\Phi_{e,3}$ from diagram 3 of Fig. 9 to $\delta\Phi_e$. As noted above Eq. (2.12), we include a factor $p(1-p)$ to adjust for the presence of a common internal-perimeter bond (the dashed bond in the figure), also we include a factor $(\sigma-1)^2/2$ for the number of ways a square can be appended to the root vertex, a factor of 2 because the dashed bond can be placed in two equivalent positions, and a factor q^1 because we have added one even site on which the wave function is nonzero. For the vertices, beginning with the root vertex and going around the square in a clockwise direction, there are the associated factors

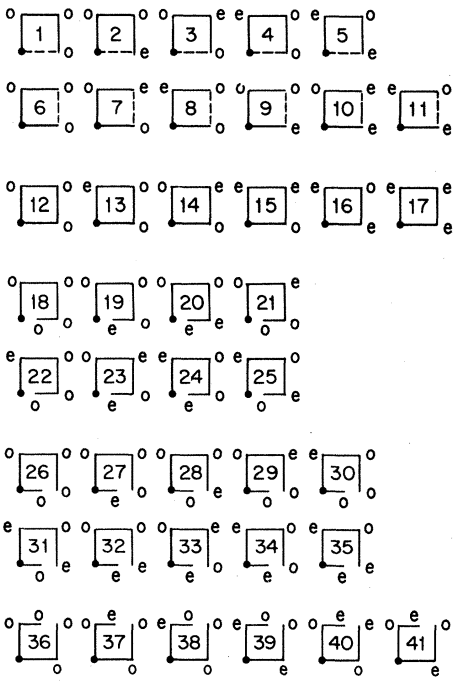

FIG. 9. Enumeration of all ways to label the diagrams of Figs. 4–6 which contribute to $\delta\Phi$. Solid circle in the lower left vertex of each square is the root vertex r.

$$[1-p+p\Sigma_o(p,q)]^{\sigma-2}\ ,\ [1-p+pq\Sigma_e(p,q)+p\Sigma_o(p)]^{\sigma-1}\ ,\ [1-p+p\Sigma_o(p,q)]^{\sigma-1}\ ,$$
$$\{[1-p+pq\Sigma_e(p,q)+p\Sigma_o(p)]^{\sigma-1}-[1-p+p\Sigma_o(p)]^{\sigma-1}\}\ , \tag{4.1}$$

where again $\Sigma(p)=\Sigma(p,1)$, so that

$$\delta\Phi_{e,3}=p(1-p)(\sigma-1)^2p^3q[1-p+p\Sigma_o(p,q)]^{2\sigma-3}$$
$$\times\{[1-p+pq\Sigma_e(p,q)+p\Sigma_o(p)]^{\sigma-1}-[1-p+p\Sigma_o(p)]^{\sigma-1}\}[1-p+yp\Sigma_e(p,q)+p\Sigma_o(p)]^{\sigma-1} \tag{4.2a}$$
$$\approx\sigma^2p^4\Sigma_e(p,q)^2\Sigma(p,q)\Sigma_o(p,q)\ , \tag{4.2b}$$

where

$$\Sigma(p,q)=\Sigma_o(p,q)+\Sigma_e(p)\ . \tag{4.3}$$

As this example shows, to evaluate $\delta\Phi$ for diagrams of Figs. 4 and 6, one takes for a vertex one of the following factors. (a) If the vertex is odd and is not followed in the sequence from the root vertex by an even vertex, it carries a factor $\Sigma_o(p,q)$ or $\Sigma_o(p,1)$. (If an odd vertex is followed by an odd vertex, then the tree attached to the vertex must provide an even neighbor. In this case Σ_o is needed.) (b) If the vertex is odd and is followed by an even vertex, then it carries a factor $\Sigma(p,q)$ or $\Sigma(p,1)$. (c) If the vertex is even, it carries a factor $\Sigma_e(p,q)$ or $\Sigma_e(p,1)$. The rule for deciding whether or not to set $q=1$ is as follows: If the wave function can propagate from the root vertex to the vertex in question, one sets the second argument of Σ equal to q, otherwise it is set equal to unity. Powers of q can be omitted, but the q dependence of the Σ factors must be kept track of in order to implement Eq. (3.11).

For the diagrams of Fig. 5, i.e., diagrams 12–17 of Fig. 9, a different procedure is needed. Here the labels of each vertex are results of the structure of the tree attached to that vertex, and have nothing to do with the sequence of vertices from the root vertex. For a typical diagram of

TABLE I. Contributions to $\delta\Phi_e$ and $\delta\Phi_o$ from diagrams Γ_k of Fig. 9. Notation: $E_q=\Sigma_e(p,q)$, $E=\Sigma_e(p)$, $O_q=\Sigma_o(p,q)$, $O=\Sigma_o(p)$, $\Sigma_q=\Sigma_o(p,q)+\Sigma_e(p)$, and $\Sigma=\Sigma_o(p)+\Sigma_e(p)$. For diagrams 1–17 we write $\delta\Phi=\sigma^2p^4G$, and for diagrams 18–41, we write $\delta\Phi=-\sigma^2p^4G$.

k	G_e	G_o	k	G_e	G_o
1	$E_qO_qO^2$	O_qO^3	2	$E_qO_q\Sigma E$	$O_qOE\Sigma$
3	$E_q{}^2\Sigma_qO_q$	$O_qOE\Sigma$	4	0	$E_qO_q\Sigma_qO$
5	0	$E_q^2\Sigma_q^2$			
6	$E_qO_q^2O$	O_qO^3	7	$E_q^2O_q\Sigma_q$	$O_qOE\Sigma$
8	0	$E_qO_q\Sigma_qO$	9	0	$E_q\Sigma_qO^2$
10	0	$E_q\Sigma_qE\Sigma$	11	0	$O_qE_q^2\Sigma_q$
12	$\frac{1}{2}E_qO_q^2O$	$\frac{1}{2}O_qO^3$	13	0	$O_qE_q\Sigma_qO$
14	$\frac{1}{2}E_q^2O_q^2$	$\frac{1}{2}O_qEO^2$	15	E_q^2EO	O_qE^2O
16	0	$\frac{1}{2}E_q^2\Sigma_qO_q$	17	$\frac{1}{2}E_q^2E^2$	$\frac{1}{2}O_qE^3$
18	$E_qO_qO^3$	O_qO^4	19	$E_qO_qOE\Sigma$	$O_qO^2E\Sigma$
20	$E_qO_qOE\Sigma$	$O_qO^2E\Sigma$	21	$E_q^2O_q\Sigma_qO$	$O_qO^2E\Sigma$
22	0	$O_q\Sigma_qE_qO^2$	23	$E_q^3\Sigma_q^2$	$O_qE^2\Sigma^2$
24	0	$O_q\Sigma_qE_qE\Sigma$	25	0	$O_qE_q^2\Sigma_q^2$
26	$O_q^2E_qO^2$	O_qO^4	27	0	$\Sigma_qE_qO^3$
28	$O_q^2E_q\Sigma E$	$O_qO^2E\Sigma$	29	$O_q^2E_q^2\Sigma_q$	$O_qO^2E\Sigma$
30	0	$O_q\Sigma_qE_qO^2$	31	0	$E_q^2\Sigma_q^2O$
32	0	$E_q\Sigma_qOE\Sigma$	33	0	$E_q\Sigma_qOE\Sigma$
34	0	$O_qE_q^2\Sigma_qO$	35	0	$E_q^3\Sigma_q^2$
36	$\frac{1}{2}E_qO_q^2O^2$	$\frac{1}{2}O_qO^4$	37	$E_q^2O_q\Sigma_qO$	$O_qEO^2\Sigma$
38	0	$E_qO_q\Sigma_qO^2$	39	0	$\frac{1}{2}E_q^2O_q^2\Sigma_q$
40	$\frac{1}{2}E_q^3\Sigma_q^2$	$\frac{1}{2}O_qE^2\Sigma^2$	41	0	$E_qO_q\Sigma_qE\Sigma$

the form of diagram 15 of Fig. 9 we label the vertices as shown in Fig. 10(a). We write the equations for the amplitudes of a zero-energy eigenfunction surrounding each vertex r, f, c, and a in turn as,

$$\psi_s+\psi_a=0,\quad \psi_f=0 \tag{4.4a}$$

$$\psi_r+\psi_c+\psi_g=0\ , \tag{4.4b}$$

$$\psi_a=0,\quad \psi_d=\psi_f=0\ , \tag{4.4c}$$

$$\psi_c+\psi_r=0,\quad \psi_b=0\ . \tag{4.4d}$$

Thus $\psi_g=0$, and we associate the factor $\Sigma_o(p,1)$ with vertex f. Since $\psi_a=0$, we associate the factor $\Sigma_e(p,1)$ with vertex a. If vertex r is chosen to be even, then the wave function can spread through site c and both sites r and c carry a factor $\Sigma_e(p,q)$. Thus for diagram 15 of Fig. 9 we have

$$\delta\Phi_e\sim\Sigma_e(p,q)^2\Sigma_e(p)\Sigma_o(p)\ , \tag{4.5}$$

as listed in Table I. If vertex r is chosen to be odd, the wave function cannot spread to site c, which therefore carries a factor $\Sigma_e(p,1)$. Note that Eqs. (4.4) do not force ψ_r to vanish. Thus for r to be an odd site, we must attach at least one odd chain to it. So, when site r is odd, it carries a factor $\Sigma_o(p,q)$. Thus, for diagram 15, we have

$$\delta\Phi_o\sim\Sigma_o(p,q)\Sigma_e(p)^2\Sigma_o(p)\ . \tag{4.6}$$

Another complicated point concerns a diagram such as 17 of Fig. 9. Suppose only the root vertex has occupied bonds attached to it, and let us label the vertices as in Fig. 10(b). Then the eigenvalue equations for zero energy lead to

$$\psi_r+\psi_b=0\ , \tag{4.7a}$$

$$\psi_a+\psi_c=0\ . \tag{4.7b}$$

These are two independent equations and therefore any eigenfunction, which has amplitude on all four vertices of the square, must be a linear combination of $\psi^{(1)}$ and $\psi^{(2)}$, where

$$\psi_i^{(1)}=\delta_{i,r}-\delta_{i,b}+\cdots\ . \tag{4.8a}$$

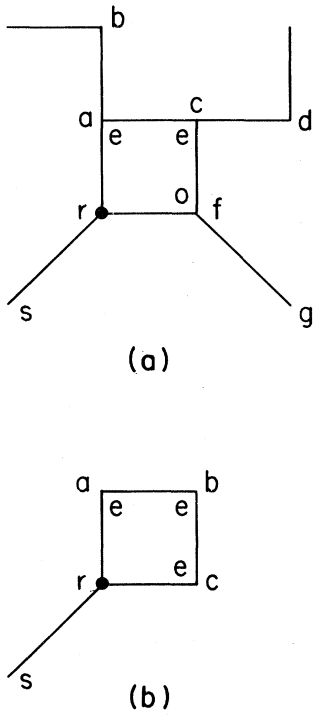

FIG. 10. Labeling of sites in diagrams 15 and 17 of Fig. 9. For the sites on the corners of the square, the labels are given outside the square and the classifications e (for even) and o (for odd) are given inside the square. Solid circle in the lower left vertex of each square is the root vertex r.

$$\psi_i^{(2)}=\delta_{i,a}-\delta_{i,c}\ , \tag{4.8b}$$

where $\psi_i^{(1)}$ extends into the rest of the cluster beyond the root. We arbitrarily consider $\psi^{(1)}$ and $\psi^{(2)}$ to be disjoint. Therefore $\delta\Phi_e$ for diagram 17 of Fig. 9 is proportional to $\Sigma_e(p,q)^2\Sigma_e(p)^2$ (which corresponds to preventing the wave function from covering sites a and c rather than to $\Sigma_e(p,q)^4$ (as it would if we allowed the eigenfunction to cover all sites on the square). Whether to call the wave functions $\psi^{(1)}$ and $\psi^{(2)}$ disjoint is really arbitrary. It will affect slightly our estimate of p^*, but will not affect our estimate of $\hat{p}$ at all. We record the results for $\delta\Phi$ obtained from Table I as follows:

$$\begin{aligned}\delta\Phi_e=&\{3\Sigma_o(q)^2\Sigma_o(1)+2\Sigma_o(q)\Sigma_o(1)^2+5\Sigma_e(q)\Sigma_o(q)^2+2\Sigma_e(1)\Sigma_o(q)\Sigma_o(1)\\&+\Sigma_o(q)\Sigma_e(1)[4\Sigma_e(q)+2\Sigma_e(1)]+2\Sigma_o(1)\Sigma_e(q)\Sigma_e(1)+\Sigma_e(q)\Sigma_e(1)^2\}\frac{p^4}{2}\sigma^2\Sigma_e(q)\\&-\{3\Sigma_o(q)^2\Sigma_o(1)^2+2\Sigma_o(q)\Sigma_o(1)^3+4\Sigma_o(q)^2\Sigma_o(1)\Sigma_e(q)+2\Sigma_o(q)^3\Sigma_e(q)\\&+2\Sigma_o(q)\Sigma_o(1)\Sigma_e(1)[2\Sigma_o(1)+\Sigma_o(q)]+\Sigma_o(q)^2[3\Sigma_e(q)^2+2\Sigma_e(q)\Sigma_e(1)+2\Sigma_e(1)^2]\\&+4\Sigma_o(q)\Sigma_o(1)\Sigma_e(q)\Sigma_e(1)+4\Sigma_o(q)\Sigma_o(1)\Sigma_e(1)^2+6\Sigma_o(q)\Sigma_e(q)^2\Sigma_e(1)+3\Sigma_e(q)^2\Sigma_e(1)^2\}\frac{\sigma^2}{2}p^4\Sigma_e(q)\ .\end{aligned} \tag{4.9a}$$

$$\delta\Phi_o=\{5\Sigma_o(q)\Sigma_o(1)^3+6\Sigma_o(q)^2\Sigma_o(1)\Sigma_e(q)+7\Sigma_o(q)\Sigma_o(1)^2\Sigma_e(1)+2\Sigma_o(q)\Sigma_o(1)^2\Sigma_e(q)$$
$$+5\Sigma_o(q)^2\Sigma_e(q)^2+8\Sigma_o(q)\Sigma_o(1)\Sigma_e(1)^2+2\Sigma_o(1)^2\Sigma_e(q)\Sigma_e(1)+8\Sigma_o(q)\Sigma_o(1)\Sigma_e(q)\Sigma_e(1)$$
$$+7\Sigma_o(q)\Sigma_e(q)^2\Sigma_e(1)+2\Sigma_o(q)\Sigma_e(q)\Sigma_e(1)^2+\Sigma_o(q)\Sigma_e(1)^3$$
$$+2\Sigma_e(q)\Sigma_e(1)^2[\Sigma_o(1)+\Sigma_e(q)+\Sigma_e(1)]\}\frac{p^4}{2}\sigma^2$$
$$-\{5\Sigma_o(q)\Sigma_o(1)^4+3\Sigma_o(q)^2\Sigma_e(q)[2\Sigma_o(1)^2+\Sigma_o(q)\Sigma_e(q)]+2\Sigma_o(q)\Sigma_o(1)^3[6\Sigma_e(1)+\Sigma_e(q)]$$
$$+2\Sigma_o(1)^3\Sigma_e(q)\Sigma_e(1)+4\Sigma_o(q)^2\Sigma_o(1)\Sigma_e(q)[\Sigma_e(q)+\Sigma_e(1)]$$
$$+5\Sigma_o(q)\Sigma_o(1)^2\Sigma_e(1)[2\Sigma_e(q)+3\Sigma_e(1)]+\Sigma_o(q)^2\Sigma_e(q)[5\Sigma_e(q)\Sigma_e(1)+2\Sigma_e(q)^2+4\Sigma_e(1)^2]$$
$$+\Sigma_o(q)\Sigma_o(1)\Sigma_e(1)[6\Sigma_e(q)^2+8\Sigma_e(q)\Sigma_e(1)+6\Sigma_e(1)^2]+4\Sigma_o(1)^2\Sigma_e(q)\Sigma_e(1)^2$$
$$+\Sigma_o(q)\Sigma_e(1)[4\Sigma_e(q)^3+2\Sigma_e(q)^2\Sigma_e(1)+4\Sigma_e(q)\Sigma_e(1)^2+3\Sigma_e(1)^3]$$
$$+\Sigma_o(1)\Sigma_e(q)\Sigma_e(1)^2[2\Sigma_e(q)+4\Sigma_e(1)]+2\Sigma_e(q)^3\Sigma_e(1)^2\}\frac{\sigma^2}{2}p^4\,. \tag{4.9b}$$

[To save space in writing these long equations, we temporarily used the abbreviations $\Sigma(q)\equiv\Sigma(p,q)$ and $\Sigma(1)\equiv\Sigma(p,1)$.]

The implementation of Eq. (3.11) including the perturbation of Eqs. (4.9) is carried out symbolically in Appendix B. We now evaluate Eq. (B10). With the use of Eqs. (3.12), (3.8), and (3.9) we have

$$\Sigma_e(p)\approx(\sigma p^*)^{-2}\,, \tag{4.10a}$$

$$\Sigma_o(p)\approx 1-(\sigma p^*)^{-2} \tag{4.10b}$$

for p near p^*. Equation (4.9) then yields

$$\delta\Phi_e=\delta\Phi_o=\frac{3(\sigma p^*)^2-5}{2\sigma^8(p^*)^6}\,, \tag{4.11}$$

and using for $p=p^*$,

$$\frac{\partial}{\partial\Lambda(p,q)}=\frac{1}{p^*}\left[\frac{\partial}{\partial\Sigma_o(p,q)}+\frac{1}{\sigma p^*}\frac{\partial}{\partial\Sigma_e(p,q)}\right], \tag{4.12}$$

we have

$$\frac{\partial[\delta\Phi_e+\sigma p^*\,\delta\Phi_o]}{\partial\Lambda(p,q)}=[-(\sigma p^*)^7-2(\sigma p^*)^6-(\sigma p^*)^5$$
$$+(\sigma p^*)^4+(\sigma p^*)^3-\tfrac{3}{2}(\sigma p^*)^2$$
$$+\sigma p^*-\tfrac{5}{2}]\frac{1}{(\sigma^7 p^6)}\,. \tag{4.13}$$

Then Eq. (B10) becomes

$$\frac{\delta p^*}{p_0^*}=\frac{\sigma^{-7}p^{-5}}{1+2\sigma p^*}[(\sigma p^*)^8+3(\sigma p^*)^7$$
$$+3(\sigma p^*)^6-2(\sigma p^*)^4+2(\sigma p^*)^3$$
$$+\tfrac{1}{2}(\sigma p^*)^2-\sigma p^*+\tfrac{5}{2}] \tag{4.14a}$$

$$\approx b/\sigma^2\,, \tag{4.14b}$$

with $b\approx 3.42$. Here we used $p^*\sigma\approx 1.421\,53$ from Eq. (3.13).

Next we evaluate the analogous correction to $\hat{p}$. From Eq. (B15) of Appendix B we have

$$\frac{\delta\hat{p}}{\hat{p}_0}=\sigma\hat{p}_0\,\delta\Phi_e\,, \tag{4.15}$$

and when $p=\hat{p}_0$, we have approximately

$$\Sigma_e(p)=-\frac{1}{\sigma\hat{p}_0}\,, \tag{4.16a}$$

$$\Sigma_o(p)=\frac{1+\sigma\hat{p}_0}{\sigma\hat{p}_0} \tag{4.16b}$$

so that

$$\delta\Phi_e=\frac{1}{2\sigma^3\hat{p}}(3\sigma\hat{p}_0+5) \tag{4.17}$$

and

$$\frac{\delta\hat{p}_0}{\hat{p}_0}=\frac{1}{2\sigma^3}(3\sigma\hat{p}_0+5)\,, \tag{4.18}$$

with $\hat{p}_0\approx-(\sigma-1)^{\sigma-1}/(\sigma)^\sigma\approx-1/(e\sigma)$. Then

$$\frac{\delta\hat{p}}{\hat{p}_0}=\frac{1}{2\sigma^2}\left[5-\frac{3}{e}\right], \tag{4.19}$$

as compared to the result for lattice animals,[10]

$$\frac{\delta K}{K}=\frac{1}{2\sigma^2}\left[5-\frac{1}{e}\right]. \tag{4.20}$$

V. CONCLUSION

We may summarize our work as follows.

(1) We have shown how to perturb the recursion relations for a Cayley tree to obtain corrections of order σ^{-2} due to square loops.

(2) We have obtained corrections to p^*, the critical con-

centration, and for $\hat{p}$, the location of the singularity on the negative, real concentration axis, for quantum percolation, as follows:

$$p^*=p_0^*\left[1+\frac{b}{\sigma^2}\right],\quad \hat{p}=\hat{p}_0\left[1+\frac{1}{2\sigma^2}\left[5-\frac{3}{e}\right]\right], \tag{5.1}$$

where the unperturbed values, denoted by the 0 subscript, are given by Eqs. (3.13) and (3.17), and b given by Eq. (4.14) is approximately 3.42.

(3) We have displayed (in Appendix A) the equivalence (within mean-field theory) between lattice animals and quantum percolation.

ACKNOWLEDGMENTS

The author thanks Professor Aharony for conversations regarding the singularities at negative p. The portion of this work done at the University of Pennsylvania was supported in part by the U.S. Office of Naval Research under Grant No. N00014-83-K-0158 and the National Science Foundation under Grant No. DMR-82-19216.

APPENDIX A: RELATION BETWEEN LATTICE ANIMALS AND QUANTUM PERCOLATION

Within mean-field theory, i.e., for the Cayley tree, we have found that

$$\Lambda(p)+p\Lambda(p)^\sigma=1 \tag{A1}$$

or

$$\Lambda(p)-1=-p\Lambda(p)^\sigma\ . \tag{A2}$$

For lattice animals on a Cayley tree, the recursion relation for the effective potential A is[10]

$$A=K(1+A)^\sigma\ , \tag{A3}$$

where K is the fugacity for bond formation. If we set $A=B-1$, then we have

$$B-1=KB^\sigma\ . \tag{A4}$$

Comparing Eqs. (A2) and (A4) we see that on the Cayley tree quantum percolation and lattice animals are equivalent if we set

$$-p=K\ . \tag{A5}$$

We note here the behavior of $\chi(p)$ for p near $\hat{p}$. Since the denominator in Eq. (2.10) is nonzero, the singularity in $\chi(p)$ will be the same as that in $\Lambda(p)$. If we call the left-hand side of Eq. (3.12a) $\Phi(\Lambda)$, then at $\hat{p}$,

$$\Phi(\Lambda,p)=1\ , \tag{A6a}$$

$$\frac{\partial\Phi(\Lambda,p)}{\partial\Lambda}=0\ , \tag{A6b}$$

where Eq. (A6b) represents $F_2=0$ from Eq. (3.16b). Expanding Eq. (A6a) in powers of $\delta p\equiv(p-\hat{p})$, we see that

$$(\delta\Lambda)^2\sim\delta p \tag{A7a}$$

or

$$\Lambda(p)\sim\Lambda(\hat{p})+\text{const}\times(p-\hat{p})^{1/2} \tag{A7b}$$

for p near $\hat{p}$. Thus

$$\chi(p)\sim\chi(\hat{p})+\text{const}\times(p-\hat{p})^{1/2}\ . \tag{A8}$$

APPENDIX B: FIRST-ORDER CORRECTIONS TO p^* AND $\hat{p}$

In this appendix we evaluate the corrections to p^* and $\hat{p}$ of order σ^{-2} in terms of the perturbation in $\delta\Phi$. We start from the equations

$$\Sigma_e(p,q)=[1-p+p\Sigma_o(p,q)]^\sigma+\delta\Phi_e\ , \tag{B1a}$$

$$\Sigma_o(p,q)=[1-p+qp\Sigma_e(p,q)+p\Sigma_o(p,1)]^\sigma -[1-p+p\Sigma_o(p,q)]^\sigma+\delta\Phi_o\ . \tag{B1b}$$

We solve Eq. (B1a) for $\Sigma_e(p,q)$ and substitute the result into Eq. (B1b), which we write in terms of $\Lambda(p,q)$ defined in Eq. (3.9). To first order in $\delta\Phi$ we obtain

$$\Phi(\Lambda)=\frac{\Lambda(p,q)-(1-p)}{p}-[\Lambda(p,1)+qp\Lambda(p,q)^\sigma]^\sigma+\Lambda(p,1)^\sigma-\sigma qp[\Lambda(p,1)+qp\Lambda(p,q)^\sigma]^{\sigma-1}\delta\Phi_e-\delta\Phi_o=0\ . \tag{B2}$$

We first calculate the corrections to p^*. For this purpose we set $\partial\Phi(\Lambda)/\partial\Lambda(p,q)=0$, so that

$$\frac{1}{p}-\sigma^2p\Lambda(p)^{\sigma-1}[\Lambda(p)+p\Lambda(p)^\sigma]^{\sigma-1}-\sigma p[\Lambda(p)+p\Lambda(p)^\sigma]^{\sigma-1}\left[\frac{\partial\delta\Phi_e}{\partial\Lambda(p,q)}\right]-\frac{\partial\delta\Phi_o}{\partial\Lambda(p,q)} -\sigma^2(\sigma-1)p^2\Lambda(p)^{\sigma-1}[\Lambda(p)+\Lambda(p)^\sigma]^{\sigma-2}\delta\Phi_e=0\ . \tag{B3}$$

Thus to locate p^* we have to solve Eqs. (B2) and (B3), which we write as

$$\Phi_0(\Lambda,p)=\frac{\Lambda(p)-(1-p)}{p}-[\Lambda(p)+p\Lambda(p)^\sigma]^\sigma+\Lambda(p)^\sigma =\gamma_1\ , \tag{B4a}$$

$$\Psi_0(\Lambda,p)=\frac{1}{p}-\sigma^2p\Lambda(p)^{\sigma-1}[\Lambda(p)+p\Lambda(p)^\sigma]^{\sigma-1}=\sigma\gamma_2\ , \tag{B4b}$$

with

$$\gamma_1=\delta\Phi_o+\sigma p\delta\Phi_e\ , \tag{B5a}$$

$$\gamma_2=\sigma^{-1}\frac{\partial\delta\Phi_o}{\partial\Lambda(p,q)}+p\frac{\partial\delta\Phi_e}{\partial\Lambda(p,q)}+\delta\Phi_e\ , \tag{B5b}$$

where we evaluated γ_1 and γ_2 for the unperturbed values of p^* and Λ and worked to leading order in $1/\sigma$. The solution to Eqs. (B4) is of the form

$$\Lambda=\Lambda_0+\delta\Lambda\ , \tag{B6a}$$

$$p^* = p_0^* + \delta p^* , \tag{B6b}$$

where Λ_0 and p_0^* are the solutions for $\delta\Phi=0$ given in Sec. III. We write

$$\Phi_0(\Lambda,p)=\Phi_0(\Lambda_0,p_0^*)+\frac{\partial\Phi_0}{\partial\Lambda}\delta\Lambda+\frac{\partial\Phi_0}{\partial p}\delta p^* , \tag{B7}$$

and similarly for Ψ_0. We find that Eq. (B4) becomes

$$[1-(\sigma p_0^*)^2]\delta\Lambda+[(\sigma p_0^*)^{-1}-1]\delta p^*=\sigma(p^*{}_0)^2\gamma_1 , \tag{B8a}$$

$$[1+2(\sigma p_0^*)]\delta\Lambda+\left[2+\frac{1}{x}\right]\delta p^*=-\sigma(p^*{}_0)^2\gamma_2 . \tag{B8b}$$

In obtaining these equations we used

$$\Lambda_0-1=-\frac{2}{\sigma}\ln(\sigma p^*{}_0)\approx-\frac{1}{\sigma^2 p^*{}_0} , \tag{B9}$$

which follows by analyzing Eqs. (3.12) and (3.13) for large σ. Thus we find

$$\frac{\delta p^*}{p^*{}_0}=\frac{p^*{}_0}{1+2\sigma p^*{}_0}\left[\sigma^2 p^*{}_0\delta\Phi_e - (1+\sigma p^*{}_0)\frac{\partial(\delta\Phi_o+\sigma p^*{}_0\delta\Phi_e)}{\partial\Lambda(p,q)}\right] . \tag{B10}$$

Now we consider the corrections to $\hat{p}$ due to $\delta\Phi$. In this case we must solve

$$\Phi_0(\Lambda,p)=\eta_1 , \tag{B11a}$$

$$\frac{\partial\Phi_0}{\partial\Lambda}(\Lambda,p)=\eta_2 , \tag{B11b}$$

where η_2 will not be needed explicitly and $\eta_1=\delta\Phi_0+\sigma p\delta\Phi_e$ evaluated at $p=\hat{p}_0$. As before, we write the solution as Eq. (B6a) and

$$\hat{p}=\hat{p}_0+\delta\hat{p} . \tag{B12}$$

Because of Eq. (B11b) the expansion of Eq. (B11a) is of the form

$$\frac{\delta\Phi_0}{\delta p}\delta\hat{p}=\eta_1 . \tag{B13}$$

We evaluate $\delta\Phi_0/\delta p$ at $p=\hat{p}$ and obtain

$$\frac{\delta\hat{p}}{\hat{p}_0}=-\frac{\sigma\hat{p}_0}{1-\sigma\hat{p}_0}(\delta\Phi_0+\sigma\hat{p}_0\delta\Phi_e) . \tag{B14}$$

Since $\delta\Phi_0+\delta\Phi_e=0$ for $q=1$, we have

$$\frac{\delta\hat{p}}{\hat{p}_0}=\sigma\hat{p}_0\delta\Phi_e . \tag{B15}$$

[1]R. Brout, Phys. Rev. 118, 1009 (1960); Phys. Rev. 122, 469 (1961).
[2]G. Horwitz and H. B. Callen, Phys. Rev. 124, 1757 (1961).
[3]M. E. Fisher and D. S. Gaunt, Phys. Rev. 133, A224 (1964).
[4]A. B. Harris, Phys. Rev. Lett. 21, 602 (1968).
[5]F. G. Vaks, A. I. Larkin, and S. A. Pikin, Zh. Eksp. Teor. Fiz. 53, 281 (1967) [Sov. Phys.—JETP 26, 188 (1968)]; 53, 1089 (1967) [26, 647 (1968)].
[6]M. G. Cottam and R. B. Stinchcombe, J. Phys. C 3, 2283 (1970).
[7]C. F. Coll III and A. B. Harris, Phys. Rev. B 4, 2781 (1972).
[8]R. B. Stinchcombe, J. Phys. C 6, 2459 (1973).
[9]D. S. Gaunt and H. Ruskin, J. Phys. A 11, 1369 (1978).
[10]A. B. Harris, Phys. Rev. B 26, 337 (1982).
[11]A. B. Harris and T. C. Lubensky, Phys. Rev. B 23, 2640 (1981).
[12]T. C. Lubensky and A. J. McKane, J. Phys. (Paris) Lett. 42, L-331 (1982).
[13]Y. Gefen, in Proceedings of Rome Conference on Disordered Systems and Localization, May, 1981 (unpublished).
[14]T. C. Lubensky and J. Isaacson, Phys. Rev. A 20, 2130 (1979).
[15]M. E. Fisher and J. W. Essam, J. Math. Phys. 2, 609 (1961).
[16]R. Raghavan and D. C. Mattis, Phys. Rev. B 23, 4791 (1981).
[17]A. B. Harris, Phys. Rev. Lett. 49, 296 (1982).
[18]A. B. Harris (to be published).
[19]This definition is motivated in analogy with the participation ratio. See D. J. Thouless, Phys. Rep. 13, 93 (1974).
[20]A. B. Harris and A. Aharony (unpublished).
[21]This procedure is described in more detail in Ref. 18.
[22]The recursion relation we use here is different from, but equivalent to, that used in Ref. 18.
[23]Y. Shapir, A. Aharony, and A. B. Harris, Phys. Rev. Lett. 49, 486 (1982).